The 8pi BGO Ball Array and Its Application to 3-Gamma PET

SUMMARY: Three-gamma positron annihilations, measured with the 8pi BGO ball array, were used to generate a PET image with a 4 cm FWHM spatial resolution.

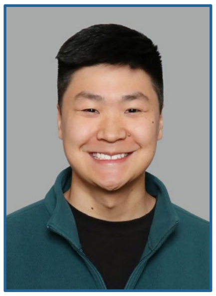

By **JOSHUA YU**[1] <joshua_yu@sfu.ca>, **KRZYSZTOF STAROSTA**[1] <starosta@sfu.ca>, **HEINZ ASCH**[2], **REBECCA GERBER**[1], **ANDREW REDEY**[3], **DAVID TAM**[2], and **ALEX WOINOSKI**[2]

[1]Department of Chemistry, Simon Fraser University, Burnaby, BC, V5A 1S6, Canada
[2]Department of Physics, Simon Fraser University, Burnaby, BC, V5A 1S6, Canada [3]School of Engineering Science, Simon Fraser University, Burnaby, BC, V5A 1S6, Canada

Joshua Yu received 3rd place in the
2025 CAP Best Overall Student Oral Presentation

Cancer is the leading cause of death in Canada, taking the lives of one in four Canadians [1]. Accurate diagnosis is an essential step in fighting this disease. Medical imaging techniques, such as Positron Emission Tomography (PET) scans, help doctors non-invasively detect and monitor cancer, guiding decisions about surgery, radiation therapy, and other treatments.

In a PET scan, the patient is injected with a drug containing a small amount of a positron-emitting radioactive isotope, known as a radiopharmaceutical. As it circulates through the body, it accumulates in areas of interest such as cancerous tissue. When the radioactive isotopes decay, they emit positrons which interact and annihilate with nearby electrons. This annihilation typically produces two gamma rays, each with an energy of 511 keV, that travel 180° apart (Fig. 1). By detecting these gamma rays, the surrounding PET scanner pinpoints where the annihilation occurred, revealing the location of cancerous tissue with millimeter precision.

In tissue, about 0.5% of positrons annihilate into three gamma rays instead of two [2]. These rare annihilations are ignored by traditional PET scans, but could provide valuable information about the local annihilation environment. For example, the rate of three-gamma annihilations is influenced by oxygen levels and tissue porosity, making it a potential early biomarker of hypoxia and other cancer-related changes [3]. However, to take advantage of this information, the locations of the three-gamma annihilations must be determined. Mapping these annihilations requires three-gamma PET imaging, which could be done alongside traditional two-gamma PET to provide complementary diagnostic information about the patient. The goal is not to replace traditional PET imaging, but to enhance it by offering additional insight into tissue properties.

Three-gamma PET image reconstruction requires locating the annihilation point from the detected gamma rays. One method uses the detection times and positions of the gamma rays to calculate the annihilation location. However, this relies on the system's timing resolution. A recent study using a PET scanner with 250 ps timing resolution achieved a spatial resolution of 8 cm [4].

In this work, an alternative energy-based approach is demonstrated using conservation of momentum. By measuring the energies and locations of the three gamma rays, the annihilation point can be reconstructed. Unlike the timing-based approach, the spatial resolution relies here on the energy resolution of the detectors. This approach is implemented using the 8pi gamma-ray spectrometer (Fig. 1), located at the Simon Fraser University Nuclear Science Laboratory (SFU NSL).

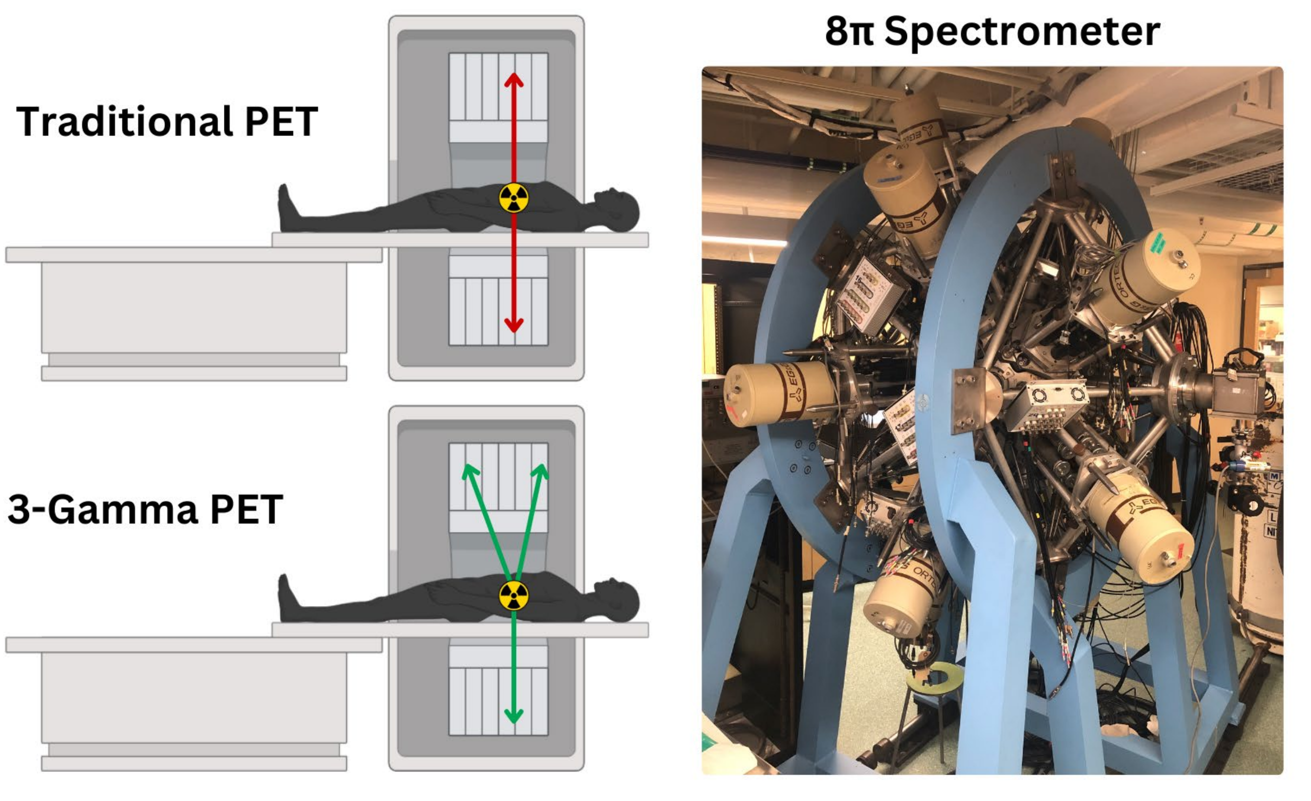

Figure 1. Illustration of a traditional PET scan and a three-gamma PET scan (left). The 8pi gamma-ray spectrometer (right).

THE 8PI GAMMA-RAY SPECTROMETER

The 8pi gamma-ray spectrometer [5] consists of 72 Bismuth Germanium Oxide (BGO) pentagon and hexagon detectors arranged in an icosahedron geometry around a central sample chamber (Fig. 2). It measures gamma-ray energies and their times of detection with high efficiency, owing to the intrinsically high gamma ray stopping power of BGO and the array's 95% solid angle coverage. Energy resolution at 661 keV is 11.7% for pentagons and 21.1% for hexagons.

The system's digital Data Acquisition System (DAQ) provides online multiplicity filtering to select events with a specific number of coincident gamma rays. When a gamma ray interacts with a BGO detector, the BGO produces a flash of light that is converted into a current pulse. This current pulse is transformed into a voltage signal whose area is related to the energy of the gamma ray, enabling energy measurements. If at least two gamma rays are detected in coincidence, the DAQ takes a snapshot of the voltage signals from all active detector channels and packages them into a single event for data analysis. This triggering requirement ensures that positron annihilations are recorded while background detections are suppressed.

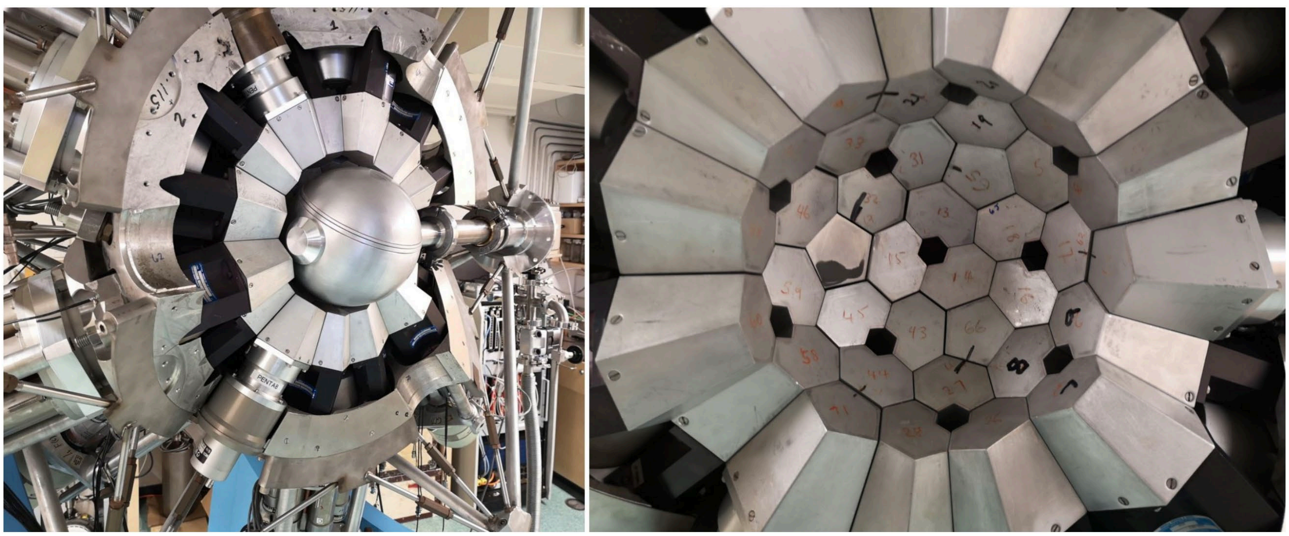

Figure 2. The 8pi gamma-ray spectrometer's BGO ball array.

THREE-GAMMA PET

In this experiment, the radioactive isotope fluorine-18 (^{18}F) is used as the source of positrons. It emits positrons with an energy of 250 keV and decays with a half-life of 110 min. ^{18}F is the most widely used PET isotope, commonly found in ^{18}F-fluorodeoxyglucose (^{18}F-FDG), a radiopharmaceutical that mimics glucose and accumulates in tissues with high metabolic activity, a characteristic of many cancers.

While ^{18}F is typically produced in hospitals using medical cyclotrons, this experiment uses a novel production method with a neutron generator [6]. A disk of polytetrafluoroethylene (Teflon) is irradiated with 14.2 MeV neutrons (n) from the generator (Fig. 3), causing the fluorine atoms naturally present in Teflon to undergo the nuclear reaction

$$^{19}\text{F} + \text{n} \rightarrow 2\text{n} + ^{18}\text{F},$$

which transforms stable fluorine-19 (^{19}F) into positron-emitting ^{18}F with a chosen activity of 450 Bq.

After irradiation, the Teflon disk is secured to the 8pi sample holder and encased in a copper sheath. The copper ensures that the emitted positrons annihilate within the sample holder, improving localization (Fig. 3). The sample is then mounted at the center of the 8pi spectrometer and measured over a period of three ^{18}F half-lives.

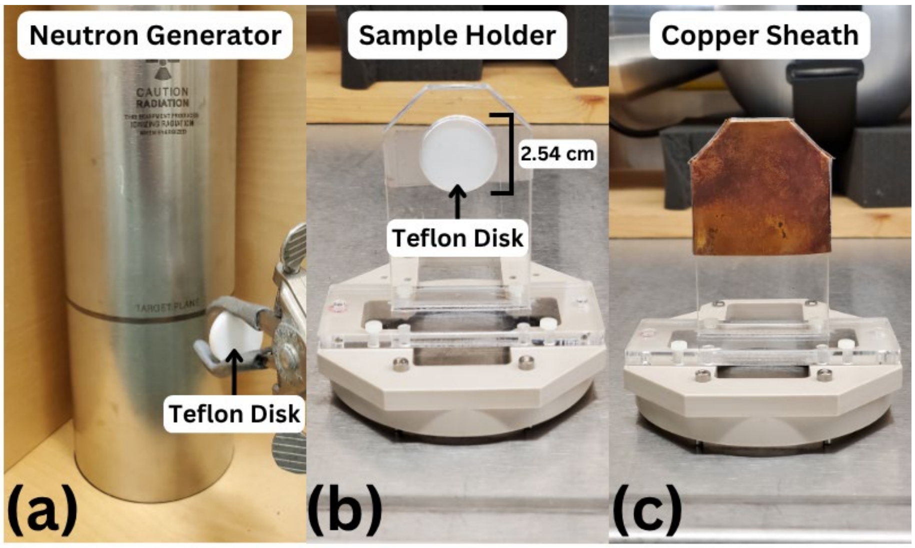

Figure 3. (a) Teflon disk secured in front of a neutron generator; (b) Irradiated Teflon disk secured in the 8pi sample holder; and (c) Irradiated Teflon disk sheathed with copper.

The collected data must be processed to isolate genuine three-gamma annihilation events. The analysis begins by identifying events in which three gamma rays are detected in coincidence. From these, only events with a total energy close to 1022 keV, the characteristic energy released in positron annihilation, are kept.

These candidate events are plotted on a ternary energy histogram (Fig. 4), which shows how the total energy is shared among the three gamma rays. Events where one gamma ray carries more than 511 keV (γ_i>0.5) are unphysical for three-gamma annihilation, as they violate conservation of linear momentum, and are excluded. Events where one gamma ray carries approximately 511 keV ($\gamma_i \approx 0.5$) likely correspond to two-gamma annihilation and are also excluded. Only events within the central region of the histogram, consistent with three-gamma annihilations, are kept.

A similar approach is applied on a ternary angle histogram (Fig. 4) to further isolate the final subset of events. Events where two gamma rays are emitted approximately 180° apart ($\theta_{ij} \approx 0.5$) are excluded. Again, only events near the center of the histogram, consistent with three-gamma annihilation, are kept.

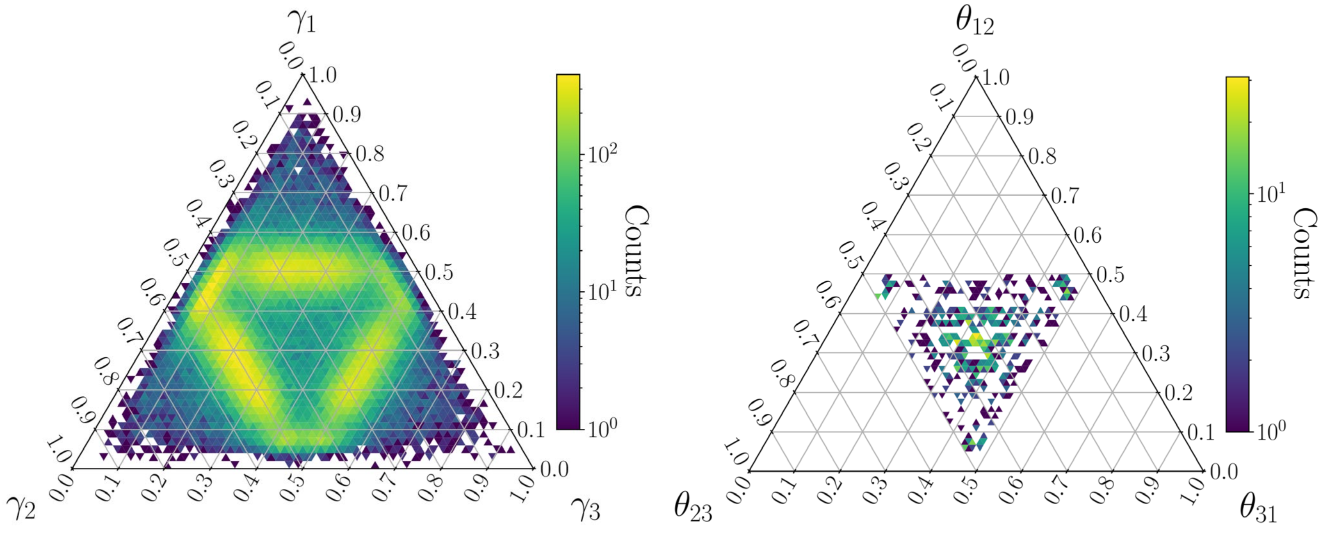

Figure 4. Ternary energy histogram (left) and ternary angle histogram (right). In the energy histogram, each axis represents a gamma ray's fraction of the total energy. In the ternary angle histogram, the interior angles between each pair of hit detector position vectors (defined from origin) are calculated. Each axis represents that interior angle's fraction of the sum of interior angles.

For each event in the final subset of data, the location of a three-gamma positron annihilation, $\vec{r} = (x, y, z)$, can be determined from solving the set of conservation of momentum equations

$$p_x = \frac{E_1}{c}\frac{x - x_1}{|(\vec{r} - \vec{r_1})|} + \frac{E_2}{c}\frac{x - x_2}{|(\vec{r} - \vec{r_2})|} + \frac{E_3}{c}\frac{x - x_3}{|(\vec{r} - \vec{r_3})|} = 0$$

$$p_y = \frac{E_1}{c}\frac{y - y_1}{|(\vec{r} - \vec{r_1})|} + \frac{E_2}{c}\frac{y - y_2}{|(\vec{r} - \vec{r_2})|} + \frac{E_3}{c}\frac{y - y_3}{|(\vec{r} - \vec{r_3})|} = 0$$

$$p_z = \frac{E_1}{c}\frac{z - z_1}{|(\vec{r} - \vec{r_1})|} + \frac{E_2}{c}\frac{z - z_2}{|(\vec{r} - \vec{r_2})|} + \frac{E_3}{c}\frac{z - z_3}{|(\vec{r} - \vec{r_3})|} = 0,$$

where E_i and $\vec{r_i} = (x_i, y_i, z_i)$ is the energy and detected location of the three gamma rays $(i = 1,2,3)$, and c is the speed of light in vacuum (Fig. 5) [7].

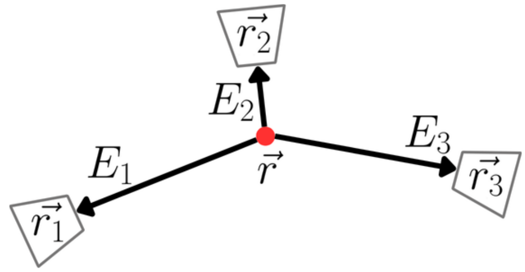

Figure 5. Schematic of three-gamma positron annihilation.

The solved locations, corresponding to 709 selected events, are plotted in Fig. 6, giving the reconstructed three-gamma PET image. The experiment was then repeated with the irradiated Teflon disk offset by -7.5 cm along the Y-axis. Following a similar analysis procedure, the reconstructed offset three-gamma PET image is plotted in Fig. 7, corresponding to 1425 selected events. The experimentally measured offset was found to be -7.4 cm ± 3.5 cm, in good agreement with the actual offset.

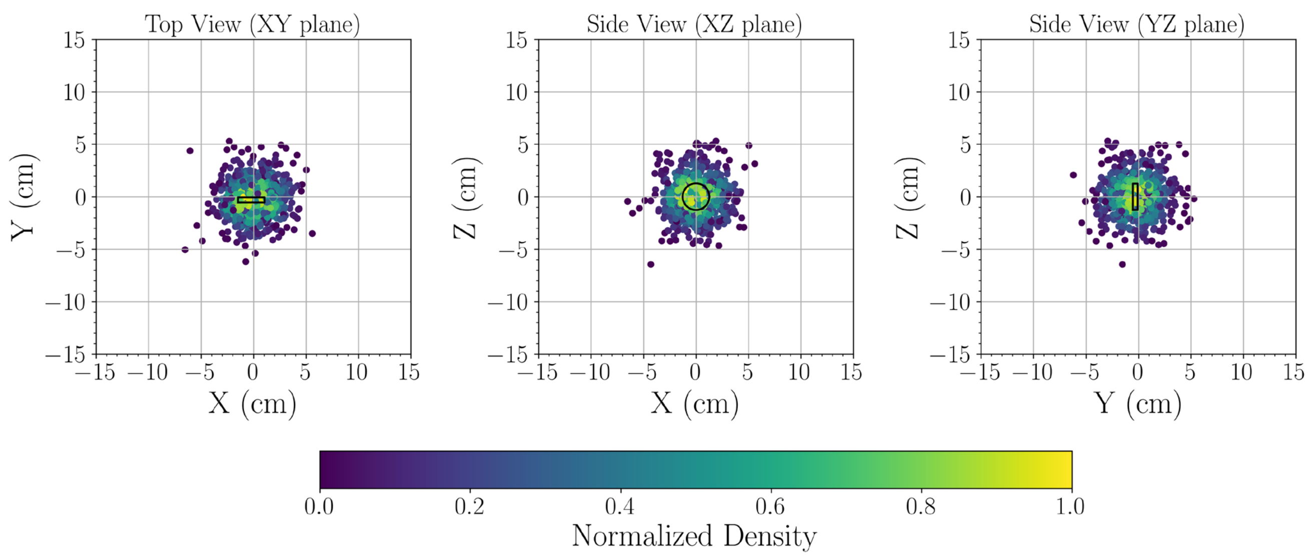

Figure 6. Three-gamma PET image of a Teflon disk measured in the center of the 8pi spectrometer. The black outline indicates the true physical size and calculated position of the irradiated Teflon disk.

The energy-based three-gamma PET image reconstruction method demonstrated here achieves a spatial resolution of 4 cm FWHM, outperforming the 8 cm resolution achieved with the timing-based approach [4]. This experiment is the first demonstration of three-dimensional image reconstruction using this energy-based approach. Owing to the high efficiency of the 8pi spectrometer, comparable statistics were obtained using much lower source activities and shorter measurement times than in previous two-dimensional energy-based three-gamma annihilation imaging experiments [7, 8]. This resulted in a four-order-of-magnitude improvement in reconstruction efficiency, defined as the number of reconstructed events divided by the total number of three-gamma annihilations.

ACKNOWLEDGEMENTS

The authors would like to thank Greg Hackman from TRIUMF, Ken van Wieren from the SFU Science Technical Centre, and Jan Tõke from JTec Instruments for their invaluable contributions with the 8pi spectrometer. This research was supported by the Natural Sciences and Engineering Research Council of Canada (NSERC) Subatomic Physics Discovery Grant Program.

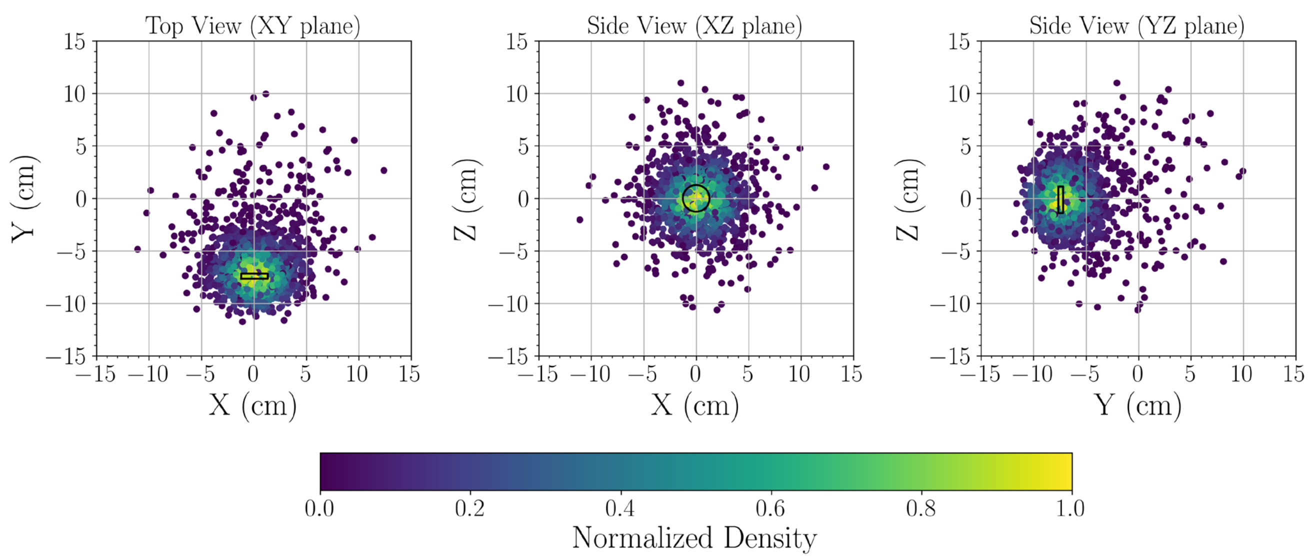

Figure 7. Three-gamma PET image of a Teflon disk offset by -7.5 cm along the Y-axis, measured in the 8pi spectrometer. The black outline indicates the true physical size and calculated position of the irradiated Teflon disk.

REFERENCES

1. D. Brenner, J. Gillis, A. Demers, L. Ellison, J. Billette, *et al.*, Projected estimates of cancer in Canada in 2024, CMAJ **196**, E615-E623 (2024).
2. B. Jasińska, B. Zgardzińska, G. Chołubek, M. Gorgol, K. Wiktor, *et al.*, Human tissues investigation using PALS technique, Acta Phys. Pol. B **48**, 1737 (2017).
3. S. Bass, S. Mariazzi, P. Moskal, and E. Stępień, Positronium physics and biomedical applications, Rev. Mod. Phys. **95**, 021002 (2023).
4. P. Moskal, A. Gajos, M. Mohammed, J. Chhokar, N. Chug, *et al.*, Testing CPT symmetry in ortho-positronium decays with positronium annihilation tomography, Nat. Commun. **12**, 5658 (2021).

5. Z. Yu, K. Starosta, C. Andreoiu, H. Asch, R. Gerber, *et al.*, A versatile digital data acquisition system for the 8π gamma-ray spectrometer, IEEE Trans. Nucl. Sci. (Early Access).
6. J. Williams, A. Chester, T. Domingo, U. Rizwan, K. Starosta, *et al.*, Neutron generator facility at SFU: GEANT4 dose rate prediction and verification, Radiat. Prot. Dosim. **171**, 313 (2016).
7. K. Kacperski, N.M. Spyrou, and F.A. Smith, Three-gamma annihilation imaging in positron emission tomography, IEEE Trans. Med. Imaging **23**, 525 (2004).
8. E. Abuelhia, K. Kacperski, and N.M. Spyrou, Three-photon annihilation in PET: 2D imaging experiments, J. Radioanal. Nucl. Chem. **271**, 489 (2007).